Macromolecules

pubs.acs.org/Macromolecules Article

Deposition of Ion-Conductive Membranes from Ionic Liquids via Initiated Chemical Vapor Deposition

Marianne Kräuter, Martin Tazreiter, Alberto Perrotta, and Anna Maria Coclite*

Cite This: *Macromolecules* 2020, 53, 7962−7969

Read Online

ACCESS | Metrics & More | Article Recommendations | Supporting Information

ABSTRACT: In this study, liquid droplets of 1-allyl-3-methylimidazolium dicyanamide have been processed by initiated chemical vapor deposition (iCVD) with a cross-linked polymer film consisting of (hydroxyethyl)methacrylate and ethylene glycol dimethacrylate to develop free-standing, ion-conductive membranes. We found that the obtained films are solids and have a conductivity of up to 18 ± 6 mS/cm, associated with the negatively charged counterion, indicating no loss of conductivity, compared to the ionic liquid in the liquid state. The membranes were conductive within a large process window and in air, thanks to the fact that the iCVD process does not affect the mobility of the anion in the ionic liquid. Furthermore, we demonstrate that varying the deposition conditions can influence the homogeneity and conductivity of the resulting membranes. The promising results of this study represent an important stepping stone on the way to novel ion-conductive membranes.

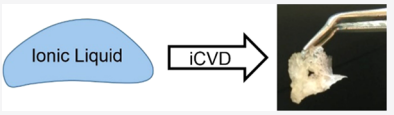

INTRODUCTION

Ionic liquids (ILs) are salts that are liquid below 100 °C, many are still in their liquid state at room temperature. ILs can be tailored to specific applications by changing sidechains or functional groups, thus contributing to their versatility.[1,2] Furthermore, their high proton or anion conductivity makes ionic liquids highly attractive for a large variety of new applications, including but not limited to their use as solvents,[3,4] electrolytes[5−7]—especially for Li-ion batteries,[8−10] for separation processes,[11,12] heat storage,[13] or utilizing them as proton-exchange membranes in fuel cells.[14−16] For many applications, however, it would be much easier to handle ILs in a solid state in the form of a membrane.

In this work, we propose the development of a solidification process for ILs that ensures retention of sufficiently high conductivity to apply the resulting ion-conductive membranes in the desired electrochemical applications. The idea is to choose an IL with vinyl bonds in either the cation or the anion and to induce free-radical polymerization, ensuring that only the part with the vinyl bonds is activated in the process and can be bound by monomers, leading to partial polymerization and thus solidification of the IL. The other ion remains unbound and thus mobile in the now solid membrane, leading to conservation of a significant amount of initial conductivity.

During radical polymerization, an initiator, I, breaks into initiator radicals, I*

$$\mathrm{I} \rightarrow \mathrm{I}^* \tag{1}$$

The reactive center is transferred from the initiator radicals to the monomers, M, and ions of the ionic liquid, $\mathrm{Ion_{IL}}$

$$\begin{aligned} \mathrm{I}^* + \mathrm{Ion_{IL}} &\rightarrow \mathrm{I} - \mathrm{Ion_{IL}}^* \\ \mathrm{I}^* + \mathrm{M} &\rightarrow \mathrm{I} - \mathrm{M}^* \end{aligned} \tag{2}$$

Successively, further monomer units react with the radicals, leading to the formation of polymer chains and polymerization of the ionic liquid

$$\begin{aligned} \mathrm{I} - \mathrm{M}^* + \mathrm{M} &\rightarrow \mathrm{I} - \mathrm{M} - \mathrm{M}^* \\ \mathrm{I} - \mathrm{Ion_{IL}}^* + \mathrm{M} &\rightarrow \mathrm{I} - \mathrm{Ion_{IL}} - \mathrm{M}^* \end{aligned} \tag{3}$$

The radical polymerization was conducted via initiated chemical vapor deposition (iCVD). It has been shown previously that iCVD does only partly polymerize the ionic liquid, resulting in better mobility of charge carriers than would be the case with complete polymerization.[17]

iCVD is a vapor deposition method to synthesize conformal thin films and shows big advantages over other conventional thin film deposition techniques since it works in the complete absence of solvents at relatively low temperatures, allowing the coating of a vast variety of substrates including liquids. Monomers, cross-linkers, and the so-called initiator molecules are introduced into the reactor chamber, where hot filaments break the initiator molecules into radicals, which then react with the monomers adsorbed on the cooled substrate surface.[18−21] Furthermore, iCVD is barely investigated in the literature for polymerizing ionic liquids,[17,22] presenting a rather novel approach for this application. It is also faster than many conventional polymerization methods and thus interesting for industrial purposes. Conventional polymerization processes that last 6,[23] 12 h[24] or even up to 2 whole days[25] are not

Received: May 28, 2020
Revised: August 21, 2020
Published: September 11, 2020

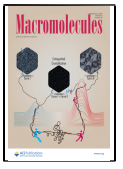

https://dx.doi.org/10.1021/acs.macromol.0c01258
Macromolecules 2020, 53, 7962−7969

uncommon in the literature for polymerization of ionic liquids. Even with the relatively short time of 3 h for polymerizing 1-vinyl-3-ethyl-imidazolium bromide and 1-vinyl-3-ethyl-imidazolium chloride, reported by Marcilla et al.,[26] the process still takes longer than a typical iCVD process.

1-Allyl-3-methylimidazolium dicynamide was chosen as the ionic liquid for this study due to its high initial conductivity and its available polymerization sites in the cation. To obtain homogeneous and stable membranes, various parameters in the iCVD process were tuned. Furthermore, the influence of deposition parameters on the conductivity of the resulting layers was investigated. The aim of this study is to showcase the potential of conductive membranes synthesized from ionic liquids via iCVD and to illustrate their stability over a large process window.

EXPERIMENTAL SECTION

Materials. (Hydroxyethyl)methacrylate (HEMA, 97%), ethylene glycol dimethacrylate (EGDMA, 98%), 1-allyl-3-methylimidazolium dicyanamide (AMID, 98.5%), and *tert*-butyl peroxide (TBPO, 98%) were purchased from Sigma-Aldrich and used as delivered without further treatment. The chemical structures of the employed chemicals can be found in Figure S1 in the Supporting Information.

Initiated Chemical Vapor Deposition (iCVD). The iCVD processes were performed in a homebuilt setup[27,28] consisting of a cylindrical vacuum chamber with a glass cover, which was evacuated by a rotary vane pump (Pfeiffer Vacuum DUO65) to a base pressure of around 1 mTorr. The substrate temperature was controlled by a chiller (Thermo Scientific Accel 500LC) connected to the bottom of the reactor, keeping the substrate temperature at 30 °C. Glass jars, which contained the chemicals for the experiment, were connected to the vacuum chamber via lines with needle valves. The jars of HEMA and EGDMA were heated to 75 and 85 °C, respectively, while the initiator TBPO was kept at room temperature. The vapor lines were heated to about 100 °C to avoid condensation. The flowrates were 0.40 ± 0.15 sccm for HEMA and 0.10 ± 0.03 sccm for EGDMA. The initiator was fed into the chamber through a separate line. Its flow rate of 0.76 sccm was set with a mass flow controller (MKS Multi Gas Controller 647C). This specific flow rate ratio of initiator, monomer, and cross-linker was chosen since it resulted in stable copolymer films. Hot nickel−chromium wires (Goodfellow, U.K.) inside the reactor near the glass lid on top were heated to about 250 °C by driving a current through them via a power supply (Heinzinger PTN 350-5) to break apart the initiator molecules and to start the polymerization process. The deposition was performed at a constant working pressure of 200 mTorr. To control the thickness of the growing polymer in situ during the deposition, a He−Ne laser beam (633 nm ThorLabs) was directed through the glass cover of the vacuum chamber onto a piece of Si wafer (Siegert Wafer, Germany) and reflected back into a detector that measures the intensity over time.

Samples. The samples produced can be roughly divided into two types: samples deposited on precoated substrates and samples deposited on bare substrates. A schematic image of the sample types is depicted in Figure 1. iCVD was employed to precoat the substrates with a polymer of HEMA and EGDMA, p(HEMA−EGDMA), of thicknesses from 50 to 200 nm. For both sample types, 5−10 μL of liquid AMID was drop-cast onto the substrates and subsequently solidified by depositing a 400−800 nm thick p(HEMA−EGDMA) top coating via iCVD. At instances, also mixtures of liquid AMID and liquid HEMA in different ratios ranging from 1:2 to 1:10 were drop-cast onto the substrates. To aid the diffusion of HEMA into the liquid AMID, prior to heating the filament (and thus prior to the polymerization process), each sample was exposed to vapors of HEMA. This process is termed as "HEMA preflow" and aided the solidification of the samples.

All samples were prepared on 2 × 2 cm^2 Si pieces (Siegert Wafer, Germany) and custom-built printed circuit boards (PCBs). The plastic base of the PCBs is partly covered by copper electrodes with a thin gold layer on top (electrode height, 36 μm). The distances between the electrodes vary from 0.4 to 1.6 mm. This variation allows one to compare and verify the validity of resistivity measurements by checking the linear relationship of resistance versus distance. One part of the PCBs was covered with a sticker during the deposition to ensure clean electrodes for resistivity measurements.

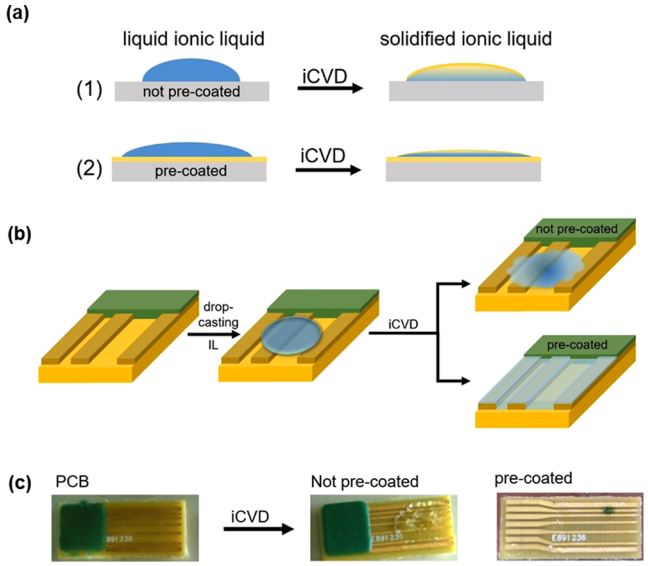

Figure 1. Solidification of AMID via iCVD. (a) Schematic depiction of the two sample types: one variant prepared on substrates precoated with p(HEMA−EGDMA) and the second on bare substrates. (b) Schematic depiction of sample preparation on printed circuit boards (PCBs): the ionic liquid was drop-cast onto either the precoated or non-precoated substrate and subsequently solidified via initiated chemical vapor deposition. (c) Photographs of a printed circuit board as purchased (left) and two printed circuit boards with a solidified ionic liquid, on a non-precoated (middle) and on a precoated sample (right). The green spot on the sample to the right is due to the aging of the sample.

Characterization Methods. Samples prepared on Si substrates were characterized via spectroscopic ellipsometry (SE), dynamic contact angle (dCA) measurements, atomic force microscopy (AFM), and Fourier-transform infrared (FTIR) spectroscopy. Layers prepared on PCBs were investigated with profilometry and electrochemical impedance spectroscopy (EIS).

The thickness of the deposited polymer layers was determined through SE (M-2000V, J.A. Woollam Co. Inc.). The polymer was modeled with a Cauchy function. In addition, the optical model included the silicon substrate and the native silicon dioxide (1.7 nm). Data acquisition took place in ambient air at three angles (65, 70, and 75°) in the wavelength range from 370 to 1000 nm.

The effect of various precoatings on the spreading of AMID on the substrate was investigated with dCA measurements. These were performed with an optical contact angle meter (KSV Instruments Ltd., Cam200) and evaluated with software CAM2008. During one dCA measurement, a liquid droplet of AMID is deposited via a syringe onto a substrate. The resulting contact angle between the liquid and the substrate surface will depend on the resulting interfacial tensions according to Young's equation.[29] In contrast to static contact angles, dCA measurements are used as the three-phase boundary moves.[30] These measurements consist of two steps: first, a drop of the liquid with increasing volume is deposited onto the substrate surface and the so-called advancing angle is measured at every step. The second step allows us to measure the receding angle. For this, the volume of the drop is gradually decreased. The receding angle is obtained at the moment right before the three-phase boundary starts to move. This means that one can obtain many advancing angles but only one receding angle with one dCA measurement. For statistical

https://dx.doi.org/10.1021/acs.macromol.0c01258
Macromolecules 2020, 53, 7962−7969

purposes, this procedure was repeated five times for each sample type. Advancing and receding contact angles give the maximum and minimum values the static contact angle can have on the surface; thus, the differences between the two can be very high.[31,32]

Solubility measurements were carried out to examine the polymerization of the solidified ionic liquid. The samples were weighed before and after suspending them in purified water, isopropanol, and toluene to determine their weight loss.

FTIR was performed in transmission mode with a Michelson interferometer (Bruker IFS 66V). All of the data was converted to absorption spectra via OPUS software. The measurement environment was kept under vacuum to minimize light scattering. Measurements were taken at different wavenumbers in the range of 500−4000 cm^{-1}. A measurement of the bare substrate was taken as a background measurement before measuring the polymer film, and the obtained polymer spectrum was divided by this substrate reference spectrum. Information about the solidified AMID was obtained in the same manner. The spectra of the polymer films were analyzed with computer program "IR_fitter".[33] This program allows for the quantification of the amount of each monomer in the copolymer film from the linear combination of the single monomer spectra. Details on this procedure can be found elsewhere.[34]

Profilometry was executed with a stylus profilometer (Bruker DektakXT) with a constant force of 3 mg over a length of 15 mm and an acquisition time of 1 min. The measurements were controlled via computer program Vision64. This technique led to the acquisition of one-dimensional height profiles of the solidified ionic liquid and was used to gain an understanding of the spreading, homogeneity, and average thickness of the membranes. The profilometry measurements were performed on coated PCBs. Its sticker was removed prior to the measurements to create a reference height of zero, namely, the height of the substrate.

Atomic force microscopy (Nanosurf easyScan 2) was conducted in noncontact mode with a PPP-NCLR-10 cantilever (NanoWorld AG, Switzerland). The obtained data was evaluated with the freely available software package Gwyddion.[35]

EIS was conducted on layers deposited on custom-built PCBs with a potentiostat Reference 600 from Gamry Instruments. For the measurements, the PCB was inserted into a counterpart plug that could be connected to the potentiostat. For two-point measurements, the working and working sense electrodes were connected to one electrode, counter and reference to the other. All resistivity measurements were performed as two-point potentiostatic EIS measurements in ambient air. Since the measurements were performed in low-humidity conditions, a two-point setup could be utilized without sacrificing accuracy for the measured values.[36] To obtain resistivity values, the measured data were fitted to appropriate electrical circuits,[37,38] as shown in Figure 2. One model was used for non-precoated samples, and the other one for precoated samples. In both models, the capacitance $C_{coating}$ represents the capacitance of the coating on the electrodes. The constant phase element and the resistance $R_{interface}$ in parallel represent the interface between the electrodes and the solidified AMID. The resistance of the solid electrolyte is noted as R_{AMID} in the drawing of the model, and this is the resistance that is obtained by the fit. The multilayer model, which was used for the precoated samples, contains an extra RC to compensate for the extra polymer layer between the electrodes on the substrate and the solidified AMID, which we want to measure. Figure 2c illustrates how the single-layer model fails to represent the data of the precoated sample, whereas the multilayer model is able to follow the measured graph.

The conductivity of the samples was calculated with eq 4. The length of the conductive layer, l, was measured with a sliding caliper, and the thickness of the conductive layer, t, between two electrodes of the PCB was measured via profilometry. b signifies the distance between the two measuring electrodes. The thickness profile was measured individually for each pair of electrodes to ensure the representative results for each electrode pair for which the resistivity measurements were performed. To make use of the simplifying assumptions of eq 4, the mean value of all measured height values of the thickness profile was chosen. The resistance, R, was measured via EIS.

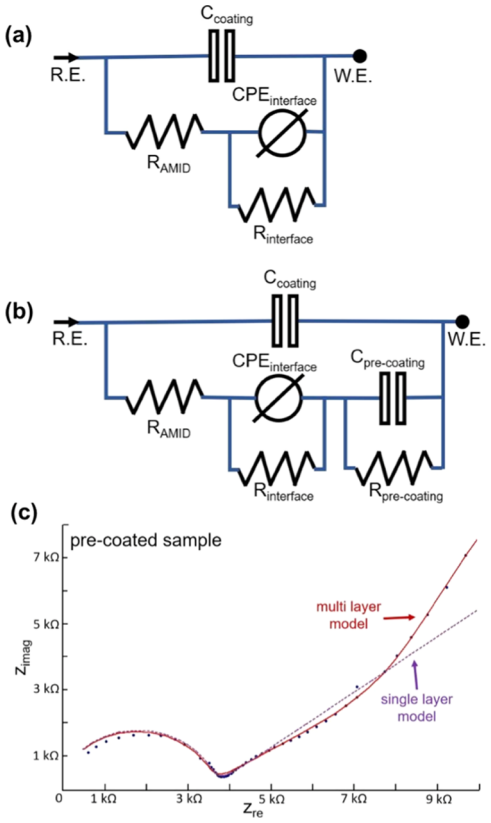

Figure 2. Fitting models used to describe the data obtained by EIS and thus obtain the resistance R_{AMID} of the solidified IL membrane. (a) EIS model for non-precoated samples, (b) EIS model for precoated samples, and (c) both fitting models were employed for an EIS measurement (depicted as the Nyquist plot) of a precoated sample to demonstrate their validity.

$$\sigma = \frac{1}{\rho} = \frac{b}{AR} = ne\mu; \quad A = tl \tag{4}$$

Multiple measurements per sample, sometimes even per electrode pair, were performed to ensure the validity of the obtained results.

RESULTS AND DISCUSSION

A first attempt to polymerize the ionic liquid was made by exposing it exclusively to the TBPO radicals in the iCVD chamber. Since this did not work at an appreciable rate, additional monomers were introduced. Solidification of the IL was obtained by adding (hydroxyethyl)methacrylate (HEMA) to the reaction feed and by employing a HEMA preflow.

This monomer was chosen due to its hydrophilicity since phase separation was to be avoided to obtain a continuous layer. Also, it has been shown that HEMA is able to penetrate ionic liquid droplets and enhances their spreading during iCVD.[39] In addition, to augment the stability of the polymer film, ethylene glycol dimethacrylate (EGDMA) was utilized as a cross-linker. To the best of our knowledge, solidification of an ionic liquid has not been shown before with this copolymer. A minimum time of HEMA preflow had to be employed during the iCVD process since the liquid AMID would not solidify otherwise, as shown in Figure 3b. A schematic of the polymer network with the incorporation of liquid AMID can be found in Figure S1 in the Supporting Information.

https://dx.doi.org/10.1021/acs.macromol.0c01258
Macromolecules 2020, 53, 7962−7969

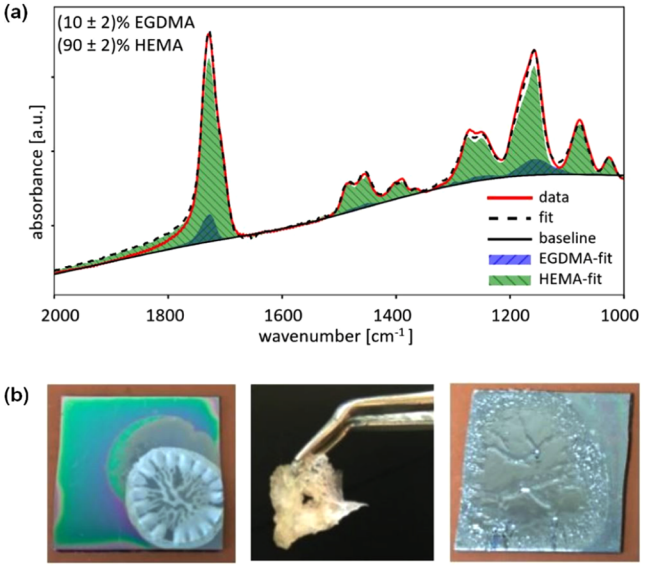

Figure 3. Investigation of solidified AMID. (a) IR spectrum of the p(HEMA−EGDMA) layer used as top coating and bottom coating. The composition of the copolymer film was calculated with IR_fitter software. (b) (From left to right) Example of a solidified AMID droplet after depositing a top coating of p(HEMA−EGDMA) via iCVD, free-standing solidified AMID, an AMID film that was not completely solidified after depositing a top coating without employing a HEMA preflow.

Figure 3a shows the FTIR spectrum of the precoating and top coating deposited by iCVD. The characteristic peaks of the HEMA and EGDMA monomers can be observed (e.g., C═O stretching absorption at 1750 cm^{-1}, CH bending at 1470−1380 cm^{-1}, and C−O stretching at 1150 cm^{-1}). From the fitting of the polymer spectrum with monomer spectra of HEMA and EGDMA, we calculated a chemical composition of 10 ± 2% EGDMA and 90 ± 2% HEMA, as evaluated via program IR_fitter.[33,34]

Figure 4a shows the advancing and receding contact angles measured on bare and precoated substrates. The angles differ significantly depending on the presence of the precoating. The fact that the advancing contact angles are higher than the receding contact angles can be attributed to the large viscosity of AMID, which leads to very slow spreading. The large contact angle hysteresis (∼20°) on the precoated substrates is caused by the surface rearrangement of the functional groups in the polymer chains. When exposed to air, the nonpolar groups of the polymer are oriented toward the surface, while when the AMID wets the surface, the polar part of the functional groups moves toward the interface.[40] This adaption of the polymer precoating to the AMID leads to significantly better wetting than on the bare Si substrate.

The varying contact angles of AMID on different thicknesses of the polymer precoating could be due to thickness-dependent swelling behavior of the polymer network. This effect has been previously shown,[41] surmising that different hydrophilicity values of the substrate and polymer layer induce differences in the swelling behavior during diffusion for different distances from the substrate and therefore for different film thickness regimes. These substrate-induced effects were found to be negligible for film thicknesses large enough (at around 100 nm). Since swelling influences other material parameters such as its density, this would account for surface tensions depending on the layer thickness and thus resulting in different contact angles. Furthermore, previous publications explored that film parameters of pHEMA are dependent on its thickness, contrary to initial expectations that the films should always present a surface of identical physiochemical characteristics, irrespective of its thickness.[42]

Figure 4b shows a comparison of the profilometry results on a sample without precoating, with 50 nm precoating, and with 200 nm precoating. The measured curves are shifted to each other for the sake of clarity. Depositing the liquid AMID onto a non-precoated substrate results in a very rough, uneven drop of solidified AMID. The substrate precoated with 50 nm p(HEMA−EGDMA) already leads to more favorable results,

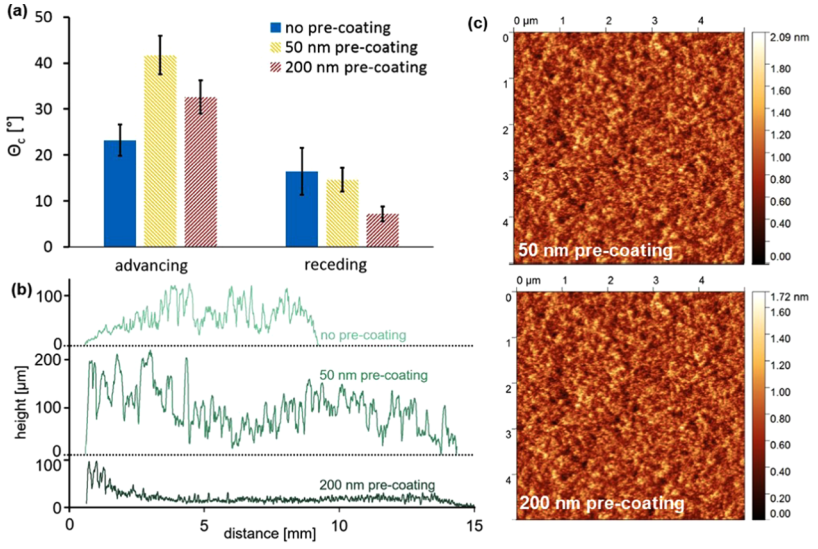

Figure 4. Measurements illustrating the spreading of liquid AMID on the substrates. (a) dCA measurements of liquid AMID on Si substrates without precoating and Si substrates with different thicknesses of p(HEMA−EGDMA) precoating, (4.b) one-dimensional height profile of solidified AMID on Si substrates and substrates precoated with p(HEMA−EGDMA), measured with profilometry, and (c) topographical AFM images of p(HEMA−EGDMA) films. In the middle is a 50 nm thick layer, and on the bottom is a 200 nm thick layer.

https://dx.doi.org/10.1021/acs.macromol.0c01258
Macromolecules 2020, 53, 7962−7969

indicating that the precoating aids the spreading of the liquid, although the layer still shows large thickness variations and appears rough. The bottom curve, which represents the sample that was precoated with 200 nm p(HEMA−EGDMA), shows a quite homogeneous layer of solidified AMID that spreads over the whole substrate and shows roughly the same thickness along the measured length. The higher thickness at a low distance in the bottom and middle curves can be attributed to edge effects at the area of the substrate, which was masked during the deposition process. Together with the results from the dCA measurements, it can be concluded that precoating substrates with a copolymer consisting of HEMA and EGDMA aid the spreading of liquid AMID on the substrate and results in more homogeneous films of solidified AMID.

In an attempt to justify why the thickness of the coating affects the homogeneity of the ionic liquid film, we measured the surface roughness of the two precoatings. The AFM measurements of a 50 and a 200 nm thick polymer layer are shown in Figure 4c. The roughness, ρ, and autocorrelation length, l_{corr}, of the p(HEMA−EGDMA) layers were calculated via a Gaussian fit of the height−height correlation function. For a 50 nm p(HEMA−EGDMA) precoating, a roughness of 0.190 ± 0.01 nm and a correlation length of 52 ± 2 nm were obtained. The respective values for the 200 nm p(HEMA−EGDMA) are ρ = 0.250 ± 0.01 nm and l_{corr} = 55 ± 2 nm. As the AFM results exhibit very similar properties for different thicknesses of p(HEMA−EGDMA), topographical effects are considered to be negligible on the spreading of AMID.

The chemical state of the solidified AMID was investigated via FTIR. Figure 5a compares the FTIR spectra of p(HEMA−EGDMA) and liquid AMID with the spectrum of solidified AMID including the p(HEMA−EGDMA) top coating. The spectrum of the liquid AMID clearly shows the C═C stretching at around 1650 cm^{-1} and the C_{sp2}−H stretching ranging from 3150 cm^{-1} to around 3000 cm^{-1}. These peaks can be assigned indistinguishably to the allyl or vinyl bonds in the AMID structure. The two peaks at 3100 cm^{-1} and a little above 3000 cm^{-1} can be attributed to the antisymmetric and symmetric stretching of CH in the CH_2 bond at the vinyl bonds of the liquid AMID. Below 3000 cm^{-1}, the absorptions of the C_{sp3}−H stretching in the CH_2 and CH_3 groups are visible, while the bending of these bonds in the same groups are visible at 1430, 1420, and 1090 cm^{-1}. The anion CN stretching absorptions are visible at 2230−2130, 1310, 940, and 760 cm^{-1}. The peaks at 1575 and 1160 cm^{-1} can be assigned to C−C antisymmetric and symmetric stretching, respectively. Most of these peaks are retained in solidified AMID, with the intensification of the absorptions of peaks corresponding to the CH_2 and CH_3 groups and the addition of C═O adsorption at 1750 cm^{-1}, coming from the p(HEMA−EGDMA) top coating. Some adsorptions of C_{sp2}−H are also visible in the spectrum of solidified AMID. These could come from the vinyl group of the imidazolium ring of AMID or from unreacted allyl groups.

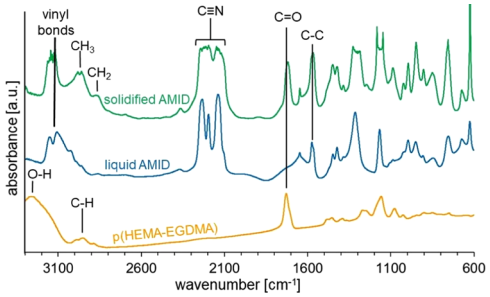

Figure 5. FTIR spectra of liquid AMID, solidified AMID with the p(HEMA−EGDMA) top coating, and the p(HEMA−EGDMA) copolymer.

Since there is no direct evidence that the allyl bonds of AMID reacted during the iCVD process, we cannot conclude that the ionic liquid was polymerized by the iCVD process. Nevertheless, the fact that the AMID is completely solidified—so well, that it could be pulled off from the substrate in instances to obtain a free-standing membrane of solidified AMID (Figure 3b)—indicates that AMID was encapsulated by the process. The presence of C≡N bonds in the solidified AMID, which only occur in the counterion that should not be altered according to our polymerization model, leads to the expectation that these groups are still mobile and conductive. The slight shift of the C═O peak compared with the curves of p(HEMA−EGDMA) and the one of the solidified AMID points toward a change in the chemical environment regarding the polymer and can be attributed to a reorientation of the dipoles with respect to each other. The small shoulder appearing below 1750 cm^{-1} in the spectrum of the copolymer is a result of two C═O peaks—one for pHEMA and one for pEGDMA—overlaying each other.[40]

Solubility tests were carried out to investigate whether AMID was actually polymerized via iCVD and thus incorporated into the p(HEMA−EGDMA) network or whether the resulting membrane is only a physical mixture of IL with the polymer network. For these tests, solidified AMID was prepared on precoated substrates, as detailed in the Experimental Section, and weighed before and after submerging them in purified water, toluene, and isopropanol for 3 h. Additional weight loss for longer time periods proved to be insignificant. The sample kept in purified water lost 67 ± 5% of its original weight during its bath, the sample submerged in toluene lost 20 ± 5%, and the sample dipped into isopropanol proved to be 34 ± 5% lighter than before. It is worth mentioning that the samples strongly delaminated and cracked during the solubility tests, especially upon immersion in water; therefore, parts of the membranes could have been lost in the solvents. As a consequence, such strong weight losses should not be considered quantitatively but only qualitatively. To compare these results to a pure physical mixture of AMID and p(HEMA−EGDMA), we drop-cast liquid AMID onto precoated Si substrates and allowed the polymer to sponge up the liquid for 1 week. The samples of this control group were then also put into solvent baths for 3 h. For each, a weight loss of 100 ± 5% was observed. The partial weight loss of solidified AMID as opposed to the complete weight loss of the samples from the control group is not conclusive about the state of polymerization but shows that the ionic liquid could be partly encapsulated during the iCVD process.

To further investigate the effect of various deposition parameters on the chemical state of AMID, FTIR spectra of different samples were compared to each other: Neither the amount of liquid AMID drop cast, duration of HEMA preflow, and thickness of top coating nor drop-casting pure AMID compared to drop-casting liquid AMID mixed with liquid HEMA yielded any effect on the polymerization of AMID (see Figure S2 in the Supporting Information).

https://dx.doi.org/10.1021/acs.macromol.0c01258
Macromolecules 2020, 53, 7962−7969

Figure 6 contains the obtained conductivity results for samples deposited with different deposition parameters to show that solid ion-conductive membranes could be obtained on a large window of conditions. Each value was averaged over multiple samples prepared in exactly the same way and whose resistivity was measured over various electrode distances. To delimit effects of the discussed deposition parameters, two strongly different values were chosen for each parameter. While the overall effect of varying these parameters is clearly visible, the trends still need to be investigated in future work. The lower value of the HEMA preflow time (10 min) was chosen since no solidification of AMID occurred without such a preflow, whereas the longer time (30 min) was chosen with general duration of each deposition in mind (see Figure 6, upper left). The chosen thicknesses of the p(HEMA−EGDMA) top coating follow similar reasoning: The lower limit (400 nm) was chosen according to the need of obtaining solidified AMID, and the upper limit (800 nm) was due to time considerations (see Figure 6, lower right). As previously mentioned, some samples were not prepared from drop-casting AMID alone but from drop-casting of mixtures of AMID and HEMA. For the AMID/HEMA drop cast, ratios of 10:1 and 2:1, respectively, were deemed to be sufficiently different from each other to yield significantly varying results (see Figure 6, upper right). Last but not least, the effect of the p(HEMA−EGDMA) precoating on the resulting conductivity of the samples was investigated (see Figure 6, lower left). The non-precoated samples exhibited higher conductivity than the ones with a 200 nm precoating.

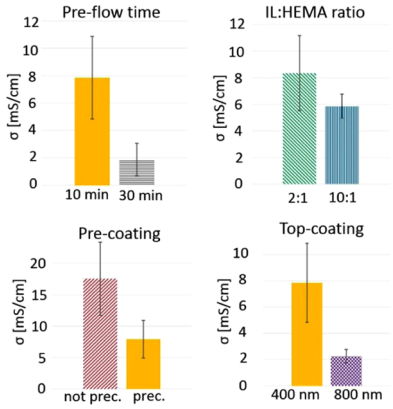

Figure 6. Effect of various deposition parameters on the resulting conductivity of the samples. The graph on the upper left shows the influence of the HEMA preflow time on the resulting conductivity of the samples. The graph on the upper right depicts the resulting conductivity of samples where instead of drop-casting pure AMID a ratio of the ionic liquid and HEMA was drop-cast. On the lower left, we see the influence of precoating the samples with p(HEMA−EGDMA) before drop-casting and subsequently solidifying AMID by comparing the result of non-precoated with that of precoated samples. The lower right graph shows the influence of the thickness of the p(HEMA−EGDMA) top coating on the conductivity of the resulting membranes.

The large error bars of the results in Figure 6 can be partly due to the large thickness variations encountered in the profilometer measurements (shown in Figure 4b) and to the error introduced when measuring the length of the conductive layer with a sliding caliper. Additionally, the cross section of the electrodes is quite small, which may be the cause of the large errors. The majority of the introduced uncertainties could be avoided by employing electrodes with a much larger cross section, which would also require different substrates, or by producing much thinner, more even layers. Recently, a way has been shown to produce pinhole-free ion-gel films enabled by iCVD in a thickness range of tens of nanometers.[43]

The conductivity of the solidified AMID was compared to a literature value of the liquid AMID that shows a conductivity of 17.0 ± 0.5 mS/cm.[44] In the best deposition conditions, the solidified AMID shows a conductivity of 18 ± 6 mS/cm, hence retaining all or nearly all of the original conductivity of the liquid IL. Lower observed conductivities for different deposition parameters could be due to the more rigid structure of p(HEMA−EGDMA) and solidified AMID compared to liquid AMID. The polymer network could hinder the movement of the anions as opposed to their movement in a liquid, even though the anion is not bound in the solidified structure. These results demonstrate that solidified AMID with good conductivity values can be synthesized within a broad processing window. However, the influence of individual processing parameters on the conductivity of the samples needs to be investigated in more detail in future work. The conductivity achieved in this study is among the highest values encountered in the literature for polymerized ionic liquids. For example, Susan et al. obtained a conductivity close to 10 mS/cm when polymerizing methyl methacrylate in 1-ethyl-3-methylimidazolium bis(trifluoromethane sulfonyl)imide.[24]

The obtained conductive solidified AMID was also compared to ion-conductive membranes consisting of copolymers of methacrylic acid (MAA), HEMA, and EGDMA, synthesized via iCVD. Such membranes have carboxylic acid groups that if exposed to water decompose into $-COO^-$ and H^+. Figure 7a shows that the highest conductivity values, namely, 8 ± 3 mS/cm, are obtained at an optimal HEMA flow rate of 0.4 sccm (corresponding to 35 ± 2% HEMA in the polymer layer). However, the measurements presented in Figure 7 were performed in very high humidity

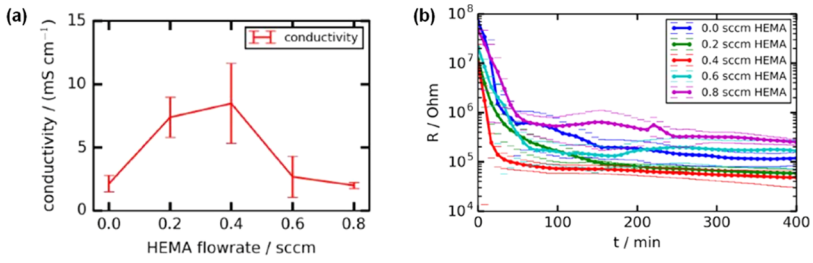

Figure 7. Conductivity of p(MAA−HEMA−EGDMA). (a) Resulting conductivity values dependent on the HEMA flow rate during the iCVD process. The resistivity measurements were performed by EIS in humidity levels ≥95%. (b) Equilibration time needed for the EIS measurements.

https://dx.doi.org/10.1021/acs.macromol.0c01258
Macromolecules 2020, 53, 7962−7969

(≥95%) and the trends in Figure 7b show how the membranes need more than 60 min of exposure to high humidity to reach a steady resistance. Such equilibration time is the time needed by the membrane to fully interact with the water to form free H^+ ions, responsible for the conductivity. Even though the conductivity mechanisms are substantially different for such membranes and those containing the ionic liquid, in one case proton conduction and in the other case anion conduction, it is worth mentioning that one advantage of employing the ionic liquid is that no equilibration time was needed since the solidified AMID was conductive also in the dry state.

To investigate the aging behavior of the samples, three samples on PCBs were prepared exactly in the same way. One had its resistance measured with EIS multiple times over the course of a month, the second was left in a dry air environment in a desiccator, and the third was placed in an argon atmosphere. The results are depicted in Figure 8. The

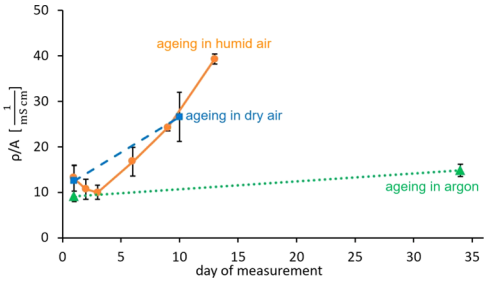

Figure 8. Measured resistivity per area of a sample kept in ambient air (humid air) vs a sample kept in a desiccator (dry air) vs a sample kept in a glovebox (argon atmosphere) to investigate aging.

resistivity results show that the samples kept in the atmosphere as well as the sample stored under dry conditions aged rapidly, whereas the sample that was kept in argon aged much slower but did age nonetheless. Each sample was measured over three different electrode pairs to validate the obtained values; exemplary measurement data can be found in Figure S3 in the Supporting Information. To detect the cause of the aging, a bare PCB, which had not corroded on its own in ambient air for 3 years, was placed in a sealed jar partially filled with water—to create a highly humid atmosphere—for 1 week without showing corrosion of the electrodes. To determine whether the materials deposited onto the PCBs are responsible for the aging, FTIR measurements of solidified AMID deposited onto silicon were performed 3 years apart from each other. The results of these measurements can be found in Figure S3 in the Supporting Information. All initially measured peaks are still present after 3 years and show no significant changes that could be attributed to aging phenomena. Since both examined components do not exhibit aging unless they are in contact with each other, our hypothesis is that the observed aging is a result of chemical reactions occurring between the copolymer and the electrodes.

CONCLUSIONS

By coating droplets of liquid AMID with a p(HEMA–EGDMA) layer via iCVD, solidified AMID membranes were obtained, which show promising conductivity values in ambient air.

Profilometry and dCA measurements proved that precoating the substrates before drop-casting the liquid IL results in better spreading of AMID and also leads to more uniform solid films. Tuned deposition parameters such as using different amounts of AMID, changing the HEMA preflow time, choosing a different thickness for the top coating vs drop-casting AMID or AMID mixed with liquid HEMA yielded no visible changes for the degree of polymerization. Precoating the samples, prior to drop-casting the IL, greatly enhanced the final membrane uniformity, despite a small decrease in conductivity.

When determining the conductivity of the produced samples from the resistivity values measured with EIS, values as high as 18 ± 6 mS/cm could be obtained in ambient air. This means that under ideal deposition conditions all of the original conductivity of liquid AMID can be retained. Although previous studies yielded comparable results at first glance, the studied ionomers p(MAA–HEMA–EGDMA) had to be measured in very high humidity (≥95%) and needed up to hours to equilibrate before good conductivity measurements could be achieved.

Several deposition parameters were largely varied, and nevertheless, conductive solid membranes could be obtained. This demonstrates the robustness of the proposed approach on a large processing window.

ASSOCIATED CONTENT

Supporting Information

The Supporting Information is available free of charge at https://pubs.acs.org/doi/10.1021/acs.macromol.0c01258.

Chemical structures of the substances used for sample synthesis (Figure S1); FTIR spectra of solidified AMID deposited with varying deposition (Figure S2); and measurements of aging samples (Figure S3) (PDF)

AUTHOR INFORMATION

Corresponding Author

Anna Maria Coclite − *Institute of Solid State Physics, NAWI Graz, Graz University of Technology, 8010 Graz, Austria;* orcid.org/0000-0001-5562-9744; Email: anna.coclite@tugraz.at

Authors

Marianne Kräuter − *Institute of Solid State Physics, NAWI Graz, Graz University of Technology, 8010 Graz, Austria*

Martin Tazreiter − *Institute of Solid State Physics, NAWI Graz, Graz University of Technology, 8010 Graz, Austria*

Alberto Perrotta − *Institute of Solid State Physics, NAWI Graz, Graz University of Technology, 8010 Graz, Austria;* orcid.org/0000-0002-7007-6153

Complete contact information is available at: https://pubs.acs.org/10.1021/acs.macromol.0c01258

Notes

The authors declare no competing financial interest.

ACKNOWLEDGMENTS

Financial support of the FWF-ProCVD project (P26993-N19) is gratefully acknowledged. Also, we acknowledge Gregor Trimmel for use of the profilometer.

REFERENCES

(1) Noble, R. D.; Gin, D. L. Perspective on Ionic Liquids and Ionic Liquid Membranes. *J. Membr. Sci.* **2011**, *369*, 1–4.

(2) Wasserscheid, P.; Welton, T. *Ionic Liquids in Synthesis*; Wasserscheid, P.; Welton, T., Eds.; Wiley-VCH, 2003.

(3) Wilkes, J. S. Properties of Ionic Liquid Solvents for Catalysis. *J. Mol. Catal. A: Chem.* **2004**, *214*, 11−17.
(4) Welton, T. Room-Temperature Ionic Liquids. Solvents for Synthesis and Catalysis. *Chem. Rev.* **1999**, *99*, 2071−2084.
(5) Lau, G. P. S.; Tsao, H. N.; Zakeeruddin, S. M.; Grätzel, M.; Dyson, P. J. Highly Stable Dye-Sensitized Solar Cells Based on Novel 1,2,3-Triazolium Ionic Liquids. *ACS Appl. Mater. Interfaces* **2014**, *6*, 13571−13577.
(6) Osada, I.; De Vries, H.; Scrosati, B.; Passerini, S. Ionic-Liquid-Based Polymer Electrolytes for Battery Applications. *Angew. Chem., Int. Ed.* **2016**, *55*, 500−513.
(7) Li, M.; Yang, L.; Fang, S.; Dong, S. Novel Polymeric Ionic Liquid Membranes as Solid Polymer Electrolytes with High Ionic Conductivity at Moderate Temperature. *J. Membr. Sci.* **2011**, *366*, 245−250.
(8) Seki, S.; Kobayashi, T.; Serizawa, N.; Kobayashi, Y.; Takei, K.; Miyashiro, H.; Hayamizu, K.; Tsuzuki, S.; Mitsugi, T.; Umebayashi, Y.; et al. Electrolyte Properties of 1-Alkyl-2,3,5-Trimethylpyrazolium Cation-Based Room-Temperature Ionic Liquids for Lithium Secondary Batteries. *J. Power Sources* **2010**, *195*, 6207−6211.
(9) Nykaza, J. R.; Savage, A. M.; Pan, Q.; Wang, S.; Beyer, F. L.; Tang, M. H.; Li, C. Y.; Elabd, Y. A. Polymerized Ionic Liquid Diblock Copolymer as Solid-State Electrolyte and Separator in Lithium-Ion Battery. *Polymer* **2016**, *101*, 311−318.
(10) Xiang, H. F.; Yin, B.; Wang, H.; Lin, H. W.; Ge, X. W.; Xie, S.; Chen, C. H. Improving Electrochemical Properties of Room Temperature Ionic Liquid (RTIL) Based Electrolyte for Li-Ion Batteries. *Electrochim. Acta* **2010**, *55*, 5204−5209.
(11) Bara, J. E.; Lessmann, S.; Gabriel, C. J.; Hatakeyama, E. S.; Noble, R. D.; Gin, D. L. Synthesis and Performance of Polymerizable Room-Temperature Ionic Liquids as Gas Separation Membranes. *Ind. Eng. Chem. Res.* **2007**, *46*, 5397−5404.
(12) Berthod, A.; Ruiz-Angel, M. J.; Carda-Broch, S. Ionic Liquids in Separation Techniques. *J. Chromatogr. A* **2008**, *1184*, 6−18.
(13) Shukla, M.; Saha, S. A Comparative Study of Piperidinium and Imidazolium Based Ionic Liquids: Thermal, Spectroscopic and Theoretical Studies. In *Ionic Liquids - New Aspects for the Future*; Kadokawa, J., Eds., 2013, Ch. 3, pp. 61−84.
(14) Ye, H.; Huang, J.; Xu, J. J.; Kodiweera, N. K. A. C.; Jayakody, J. R. P.; Greenbaum, S. G. New Membranes Based on Ionic Liquids for PEM Fuel Cells at Elevated Temperatures. *J. Power Sources* **2008**, *178*, 651−660.
(15) Gohil, J. M.; Karamanev, D. G. Novel Approach for the Preparation of Ionic Liquid/Imidazoledicarboxylic Acid Modified Poly(Vinyl Alcohol) Polyelectrolyte Membranes. *J. Membr. Sci.* **2016**, *513*, 33−39.
(16) Díaz, M.; Ortiz, A.; Ortiz, I. Progress in the Use of Ionic Liquids as Electrolyte Membranes in Fuel Cells. *J. Membr. Sci.* **2014**, *469*, 379−396.
(17) Bradley, L. C.; Gupta, M. Encapsulation of Ionic Liquids within Polymer Shells via Vapor Phase Deposition. *Langmuir* **2012**, *28*, 10276−10280.
(18) Gleason, K. K. *CVD Polymers: Fabrication of Organic Surfaces and Devices*; Gleason, K. K., Ed.; Wiley-VCH: 2015.
(19) Martin, T. P.; Lau, K. K. S.; Chan, K.; Mao, Y.; Gupta, M.; Shannan O'Shaughnessy, W.; Gleason, K. K. Initiated Chemical Vapor Deposition (ICVD) of Polymeric Nanocoatings. *Surf. Coat. Technol.* **2007**, *201*, 9400−9405.
(20) Ranacher, C.; Resel, R.; Moni, P.; Cermenek, B.; Hacker, V.; Coclite, A. M. Layered Nanostructures in Proton Conductive Polymers Obtained by Initiated Chemical Vapor Deposition. *Macromolecules* **2015**, *48*, 6177−6185.
(21) Lau, K. K. S.; Gleason, K. K. Initiated Chemical Vapor Deposition (ICVD) of Poly(Alkyl Acrylates): An Experimental Study. *Macromolecules* **2006**, *39*, 3688−3694.
(22) Bradley, L. C.; Gupta, M. Copolymerization of 1-Ethyl-3-Vinylimidazolium Bis(Trifluoromethylsulfonyl)Imide via Initiated Chemical Vapor Deposition. *Macromolecules* **2014**, *47*, 6657−6663.
(23) Yoshizawa, M.; Ogihara, W.; Ohno, H. Novel Polymer Electrolytes Prepared by Copolymerization of Ionic Liquid Monomers. *Polym. Adv. Technol.* **2002**, *13*, 589−594.
(24) Susan, M. A. B. H.; Kaneko, T.; Noda, A.; Watanabe, M. Ion Gels Prepared by in Situ Radical Polymerization of Vinyl Monomers in an Ionic Liquid and Their Characterization as Polymer Electrolytes. *J. Am. Chem. Soc.* **2005**, *127*, 4976−4983.
(25) Yuan, J.; Schlaad, H.; Giordano, C.; Antonietti, M. Double Hydrophilic Diblock Copolymers Containing a Poly(Ionic Liquid) Segment: Controlled Synthesis, Solution Property, and Application as Carbon Precursor. *Eur. Polym. J.* **2011**, *47*, 772−781.
(26) Mecerreyes, R.; Marcilla, R.; Alberto Blazquez, J.; Pomposo, J. A.; Rodriguez, J. Tuning the Solubility of Polymerized Ionic Liquids by Simple Anion-Exchange Reactions. *J. Polym. Sci., Part A: Polym. Chem.* **2004**, *42*, 208−212.
(27) Christian, P.; Ehmann, H. M. A.; Werzer, O.; Coclite, A. M. Wrinkle Formation in a Polymeric Drug Coating Deposited via Initiated Chemical Vapor Deposition. *Soft Matter* **2016**, *12*, 9501−9508.
(28) Perrotta, A.; Christian, P.; Jones, A. O. F.; Muralter, F.; Coclite, A. M. Growth Regimes of Poly(Perfluorodecyl Acrylate) Thin Films by Initiated Chemical Vapor Deposition. *Macromolecules* **2018**, *51*, 5694−5703.
(29) Young, T. An Essay on the Cohesion of Fluids. *Philos. Trans. R. Soc. Lond.* **1805**, *95*, 65−87.
(30) Marmur, A. Thermodynamic Aspects of Contact Angle Hysteresis. *Adv. Colloid Interface Sci.* **1994**, *50*, 121−141.
(31) Chibowski, E. On Some Relations between Advancing, Receding and Young's Contact Angles. *Adv. Colloid Interface Sci.* **2007**, *133*, 51−59.
(32) Gao, L.; McCarthy, T. J. Contact Angle Hysteresis Explained. *Langmuir* **2006**, *22*, 6234−6237.
(33) Tazreiter, M.. *IR_fitter*, Github: https://github.com/MartinTa/IR_fitter. 2017.
(34) Tazreiter, M.; Christian, P.; Schennach, R.; Grießer, T.; Coclite, A. M. Simple Method for the Quantitative Analysis of Thin Copolymer Films on Substrates by Infrared Spectroscopy Using Direct Calibration. *Anal. Methods* **2017**, *9*, 5266−5273.
(35) Necas, D.; Klapetek, P.. *Gwyddion*, Department of Nanometrology, Czech Metrology Institute http://gwyddion.net/, 2020.
(36) Lee, C. H.; Park, H. B.; Lee, Y. M.; Lee, R. D. Importance of Proton Conductivity Measurement in Polymer Electrolyte Membrane for Fuel Cell Application. *Ind. Eng. Chem. Res.* **2005**, *44*, 7617−7626.
(37) Amirudin, A.; Thieny, D. Application of Electrochemical Impedance Spectroscopy to Study the Degradation of Polymer-Coated Metals. *Prog. Org. Coat.* **1995**, *26*, 1−28.
(38) GAMRY. Basics of Electrochemical Impedance Spectroscopy. *Appl. Note AC* **2010**, *1*, 1−17.
(39) Haller, P. D.; Frank-Finney, R. J.; Gupta, M. Vapor-Phase Free Radical Polymerization in the Presence of an Ionic Liquid. *Macromolecules* **2011**, *44*, 2653−2659.
(40) Unger, K.; Resel, R.; Coclite, A. M. Dynamic Studies on the Response to Humidity of Poly (2-Hydroxyethyl Methacrylate) Hydrogels Produced by Initiated Chemical Vapor Deposition. *Macromol. Chem. Phys.* **2016**, *217*, 2372−2379.
(41) Muralter, F.; Perrotta, A.; Coclite, A. M. Thickness-Dependent Swelling Behavior of Vapor-Deposited Smart Polymer Thin Films. *Macromolecules* **2018**, *51*, 9692−9699.
(42) Lyndon, M. J. Synthetic Hydrogels As Substrata for Cell Adhesion Studies. *Br. Polym. J.* **1986**, *18*, 22−27.
(43) Liu, A. *Mechanically Flexible Vapor-Deposited Polymeric Thin Films for Electrochemical Devices*; Massachusetts Institute of Technology, 2017.
(44) IoLiTec Ionic Liquids Technologies GmbH. 1-Allyl-3-methylimidazoliumdicyanamide, >98% | IoLiTec. https://iolitec.de/products/ionic_liquids/catalogue/imidazolium-based/il-0240-hp. (accessed May 2, 2020).

https://dx.doi.org/10.1021/acs.macromol.0c01258
Macromolecules 2020, 53, 7962−7969